Solid State Science and Technology, Vol. 15, No 1 (2007) 156-162
ISSN 0128-7389

PHASE DIAGRAM AND DIELECTRIC PROPERTIES OF MATERIALS IN Bi_2O_3-ZnO-Ta_2O_5 SYSTEM

C.C. Khaw, C.K. Lee, Z. Zainal, Y.P. Tan and Y.H. Taufiq-Yap

Chemistry Department, Universiti Putra Malaysia
43300 Serdang, Selangor

ABSTRACT

The subsolidus phase diagram of the system Bi_2O_3-ZnO-Ta_2O_5 in the region of the cubic pyrochlore phase has been determined at 1050°C. This phase forms a solid solution area that includes the ideal composition P, $Bi_3Zn_2Ta_3O_{14}$. Possible solid solution mechanisms for the cubic pyrochlore phase are proposed. Density measurements of Zn deficient solid solutions were carried out in order to determine the possible solid solution formation mechanisms. The general formula of the solid solutions is proposed to be $Bi_{3+y}Zn_{2-x}Ta_{3-y}O_{14-x-y}$, based on the mechanisms of Zn/oxide ion vacancies and variable Bi/Ta ratio. Solid solution series at x = 0 and y = 0 were investigated using impedance spectroscopy for their dielectric properties. These materials appeared to be dielectric. $Bi_3Zn_2Ta_3O_{14}$ has ε' of 42 at 30°C and 1 MHz; ε' for the solid solutions range from 39 to 65. A high degree of dispersion on the permittivity at low frequencies (<1 kHz) and temperatures above 600°C is apparent.

INTRODUCTION

The pyrochlore structure has received careful attention for a long time because of its high-temperature stability and the various potential domains of applications of materials that adopt this structure [1,2]. Oxide pyrochlores have the general formula $A_2B_2O_6O'_{1-\delta}$ (where A is a trivalent cation and B is a tetravalent cation): the formula illustrates the well-known ability of the structure to accommodate oxygen nonstoichiometry. The space group of ideal pyrochlore structure is Fd3m and there are eight molecules per unit cell (Z=8) [3]. Studies of the cation distributions in bismuth zinc antimonates have revealed that Zn cations occupy both the A and B sites of the pyochlore structure, and the composition $Bi_{1.5}ZnSb_{1.5}O_7$ can be represented by the structural formula $(Bi_{1.5}Zn_{0.5})(Sb_{1.5}Zn_{0.5})O_7$ [4]. Bismuth-based pyrochlores have been found to be of interest for low-fire high frequency dielectric applications. In contrast to conventional microwave dielectric materials, e.g. $Ba(Mg_{1/3}Ta_{2/3})O_3$ and Zr(Sn, Ti)O_4 that require high sintering temperatures (T sinter >1600K) the low sintering temperatures of bismuth pyrochlores (T sinter ≤ 1400K) and dielectric properties with low losses (tan δ ~10^{-4}) and dielectric constants up to 150 make them promising candidates for cofired decoupling capacitors in multichip module packaging applications [4,5]. Bi-pyrochlore dielectrics are utilized in a variety of integrated devices in thick- and thin-film form. These devices include LTCC (low temperature cofire ceramics) integrated NPO (negative, positive, but almost zero temperature coefficient of capacitance) capacitors,

Corresponding Author: khaw.cc@gmail.com

Solid State Science and Technology, Vol. 15, No 1 (2007) 156-162
ISSN 0128-7389

thin-film decoupling capacitors, band-pass and low-pass filters, and RC surface-mount components [6].

Recently Bi_2O_3-ZnO-Ta_2O_5 (BZT) system has attracted much attention as new materials with promising microwave properties. α (cubic) BZT has a higher dielectric constant than β (pseudo-orthorhombic) phase, similar to the BZN system [7]. Dielectric properties of the two primary phases in BZT were measured using wave-guide transmission, ring resonator, resonant post and split cavity at microwave frequencies [8].

Most of the studies in BZT system focused on materials on the join between the α and β phase. There is thus far, relatively little information on solid solutions of cubic pyrochlores in the Bi_2O_3-ZnO-Ta_2O_5 ternary system. We report here a subsolidus phase diagram of the system Bi_2O_3-ZnO-Ta_2O_5 in the region of the cubic pyrochlore, and electrical properties of selected solid solutions of cubic $Bi_3Zn_2Ta_3O_{14}$ pyrochlore.

EXPERIMENTAL DETAILS

Bismuth zinc tantalate materials were prepared using Bi_2O_3 (99.9%, Aldrich), ZnO (99%, Merck), and Ta_2O_5 (99.993%, Alfa-Aesar) as reagents via solid-state reactions. Bi_2O_3 was dried at 300°C for 1-2 hours prior to weighing while ZnO and Ta_2O_5 were dried at 600°C for 2-3 hours. Compositions were weighed (3-4g total), mixed with acetone in an agate mortar, dried and fired in platinum foil boats at 1050°C and duration of 2 days, with intermediate regrinding. Weight-loss check showed no significant loss through volatilization for the materials used. The samples were analyzed by X-ray powder diffraction (Shimadzu diffractometer XRD 6000, CuKα radiation). Routine analysis was carried out at scan rate of 2^0/minute in the 2θ ranges of 10^0 to 70^0. Data for cell parameters determination were collected at scan rate of 0.1^0/minute. Chekcell Refinement Programme was used to obtain cell parameters. Density measurements were carried out using an ACCUPY pycnometer with N_2 purge; displacement of gas from the 1cm3 porous chamber yielded the volume of powdered samples. Electrical properties were determined by ac impedance spectroscopy using a Hewlett-Packard Impedance Analyzer HP 4192A in the frequency range of 5 Hz to 13 MHz. Pellets were cold-pressed and sintered at synthesis temperature overnight prior to electrical measurements. Gold paste electrodes were then fired on at 200°C-600°C. Measurements were made from room temperature to 850°C by incremental steps of 50°C on a heating cycle with 30 min equilibration time. The samples were left overnight at ~ 850°C and a cooling cycle performed the next day.

RESULTS AND DISCUSSION

Phase diagram

Approximately 90 samples were synthesized with final reaction temperature of 1050°C for 24 hours in the region of the cubic pyrochlore phase.

Partial phase diagram was constructed from these samples, as shown in Fig. 1. The cubic pyrochlore solid solutions form over an area of compositions, with ZnO varying from 21 to 25 mol%, including the ideal stoichiometry, P that forms the edge of the solid solution area. Since the solid solutions form over a compositional area, two

Corresponding Author: khaw.cc@gmail.com

compositional variables are needed to describe them. The first variable proposed is to describe a solid solution line passing through the ideal stoichiometry, P to Zn-deficient compositions. This is shown on an expanded scale in Fig. 2. P, shown as a large circle, forms the edge of the solid solution area and the Zn-deficient solid solutions form a line through P to sample 40. The second variable is Bi : Ta ratio, from sample 86 to 85 (at constant 21 mol% ZnO) as shown in Fig. 2.

There are a few possibilities for the compensation of Zn deficiency (first variable), similar to that of the Nb system [9]. The first possibility is to create equal numbers of zinc and oxygen vacancies, which could be described with the formula $Bi_3Zn_{2-x}Ta_3O_{14-x}$. A second possibility can be described by the formula $Bi_{3+a/2}Zn_{2-2a}Ta_{3+a/2}O_{14}$, in which Zn deficiency is compensated by excess of Bi and/or Ta, but with constant oxygen content. A third possibility is that Zn deficiency is compensated by equal numbers of Bi/Ta so as to maintain the total cation content and therefore with interstitial oxygens, represented by the formula $Bi_{3+b/2}Zn_{2-b}Ta_{3+b/2}O_{14+b}$.

To distinguish the three possibilities, density measurements were carried out. The results together with calculated densities for the three mechanisms, based on the lattice parameters, are shown in Fig. 3. Experimental density coincided with that of mechanism 1, in which there is a decrease in density with decreasing ZnO content.

The solid solution area in Figs. 1 and 2 also has variable Bi : Ta ratio (composition 86 to 85 in Fig. 2). These compositions can be described in terms of a one-to one replacement of Bi and Ta, together with, presumably, a variation in oxygen content to achieve charge balance. Given that mechanism 1 shows the likelihood of variable oxygen content associated with variable Zn content, it is likely that a variable in oxygen content can provide the charge balance required to compensate the variation in Bi : Ta ratio. The solid solution area in the phase diagram can therefore be described by a combination of $Bi_3Zn_{2-x}Ta_3O_{14-x}$ and $Bi_{3+y}Zn_2Ta_{3-y}O_{14-y}$, to yield the formula of $Bi_{3+y}Zn_{2-x}Ta_{3-y}O_{14-x-y}$, $-0.20 \leq y \leq 0.16$ and $0.00 \leq x \leq 0.40$.

Corresponding Author: khaw.cc@gmail.com

Solid State Science and Technology, Vol. 15, No 1 (2007) 156-162
ISSN 0128-7389

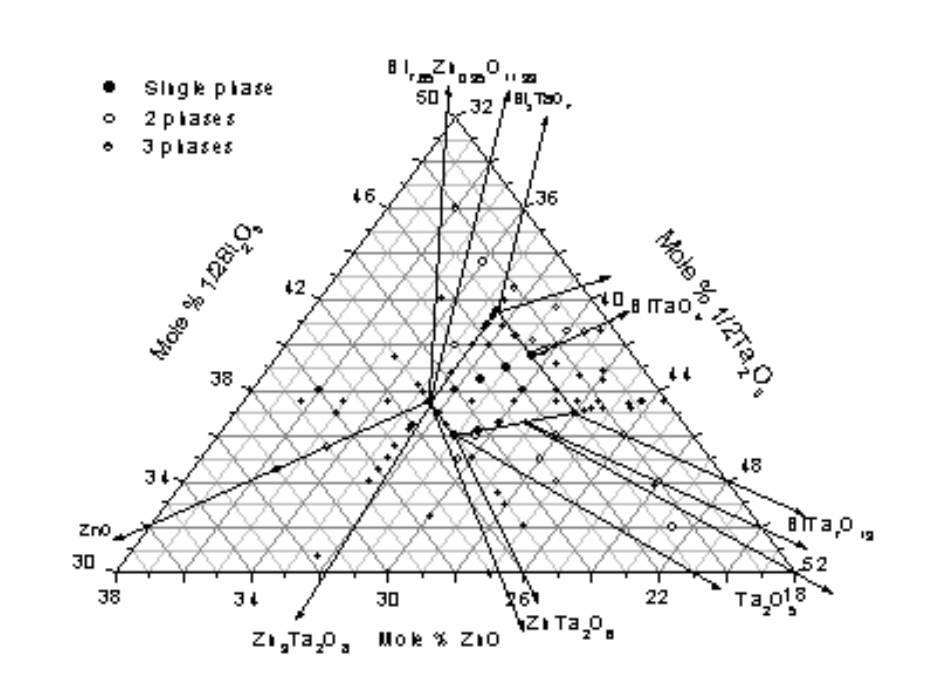

Figure 1: Partial subsolidus phase diagram at 1050°C of the Bi_2O_3-ZnO-Ta_2O_5 ternary system

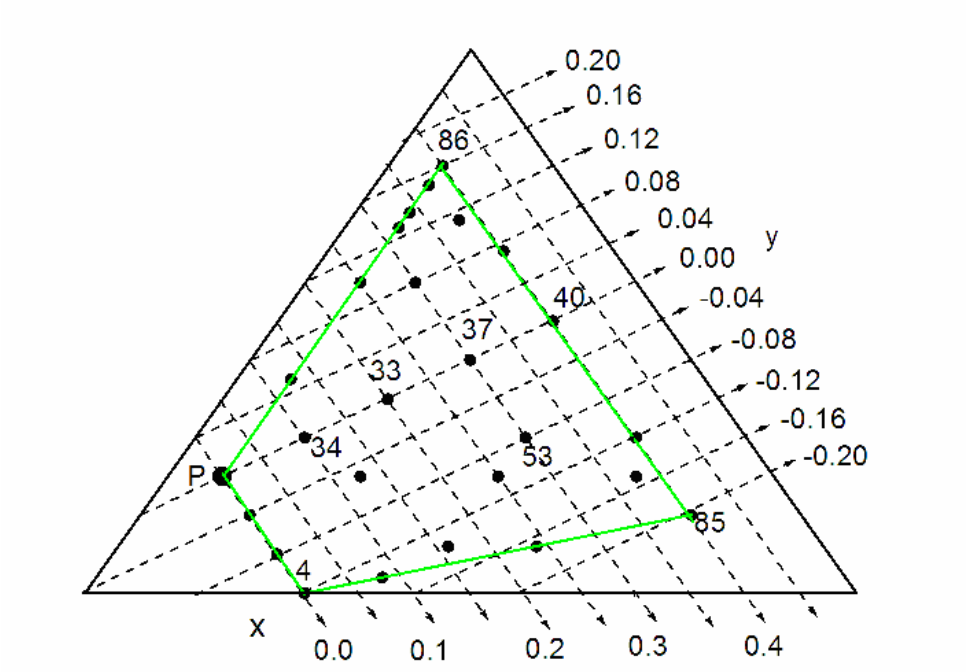

Figure 2: Expanded cubic pyrochlore solid solution area superposed on the compositional grid with x and y as variables in the formula, $Bi_{3+y}Zn_{2-x}Ta_{3-y}O_{14-x-y}$

Corresponding Author: khaw.cc@gmail.com

Solid State Science and Technology, Vol. 15, No 1 (2007) 156-162
ISSN 0128-7389

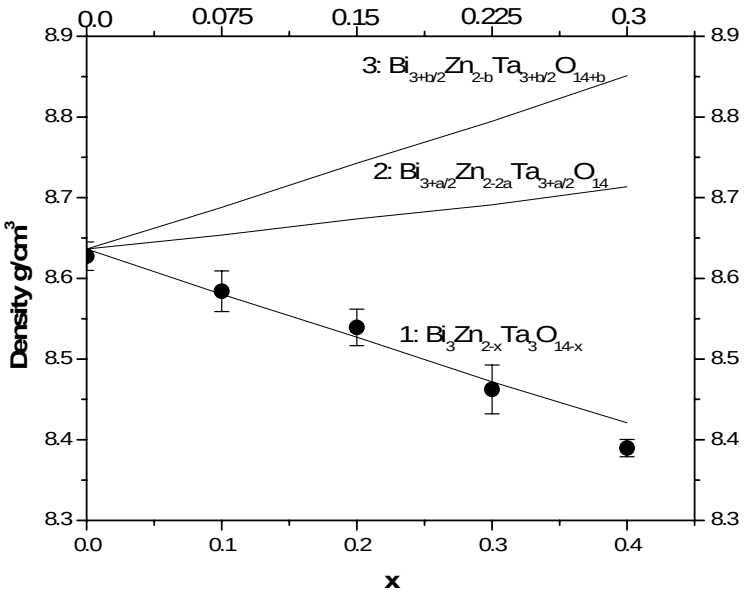

Figure 3: Density measurements of Zn-deficient series and calculated density based on lattice parameters.

Electrical Properties

Impedance measurements over the range of 5-13 MHz were performed on single-phase pyrochlore solid solutions of $Bi_{3+y}Zn_2Ta_{3-y}O_{14-y}$ (x = 0) and $Bi_3Zn_{2-x}Ta_3O_{14-x}$ (y = 0). The dielectric properties of the materials were investigated at various frequencies and temperatures. A high degree of dispersion of the permittivity, ε' of $Bi_3Zn_2Ta_3O_{14}$ ceramic at low frequencies (<1 kHz) and temperatures above 600°C is evident (Fig. 4). These behaviours are similar to those observed in $Bi_3Zn_2Sb_3O_{14}$ ceramic. They are commonly seen in dielectric materials, in which a conduction mechanism of the hopping type is present [10]. The dispersions may be associated with the presence of atomic defects in the structure in which a large number of unoccupied atomic sites is exhibited. This is seen in cubic pyrochlore where oxygen vacancies are an intrinsic defect [11]. ε' decreased with increasing frequency probably because the jumping frequency of electric charge carriers cannot follow the alternation of applied ac electric field beyond a certain critical frequency [12]. Fig. 5 shows the variation of permittivity with composition for the two solid solution series and ε' varies from 39 to 65. Permittivity values are, in general, higher than those reported for bismuth zinc antimonate (BZS) but lower than those of bismuth zinc niobate (BZN) ceramics [4,12].

Corresponding Author: khaw.cc@gmail.com

Solid State Science and Technology, Vol. 15, No 1 (2007) 156-162
ISSN 0128-7389

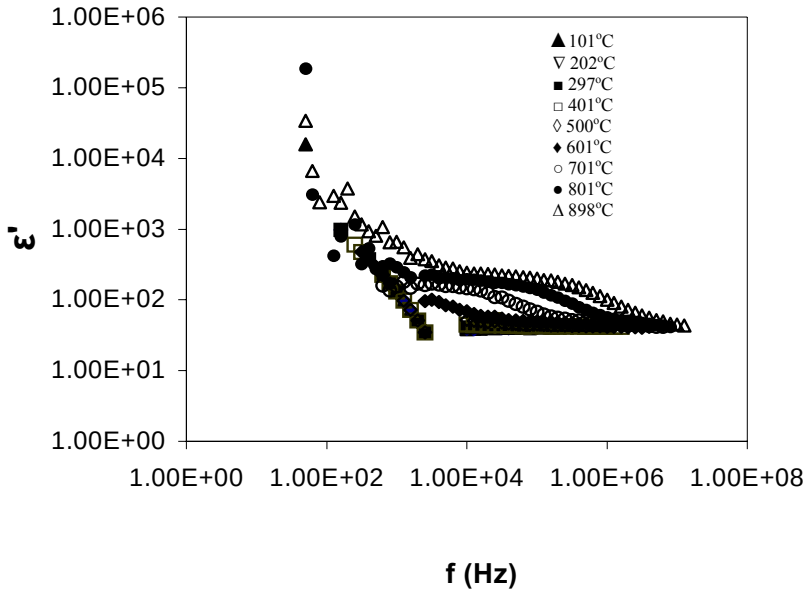

Figure 4: Real part of complex permittivity as a function of frequency at several temperatures

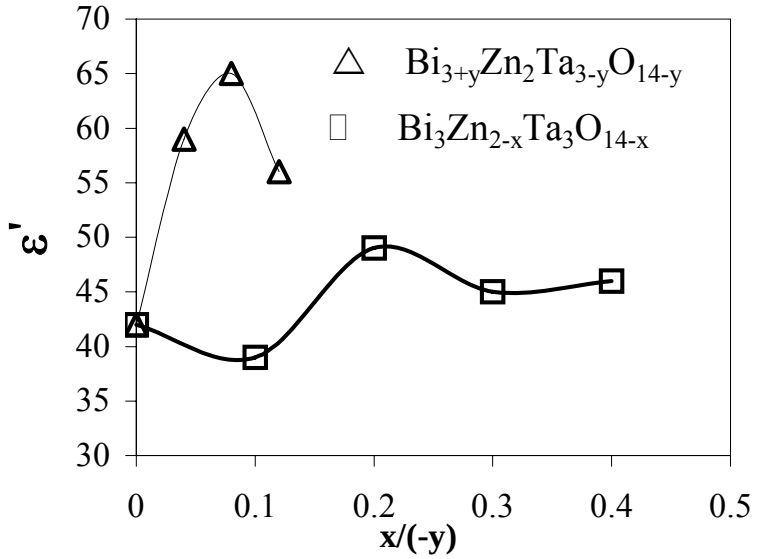

Figure 5: Real part of complex permittivity (1 MHz at 650°C) of $Bi_{3+y}Zn_{2-x}Ta_{3-y}O_{14-x-y}$ at x = 0 and y = 0

Corresponding Author: khaw.cc@gmail.com

Solid State Science and Technology, Vol. 15, No 1 (2007) 156-162
ISSN 0128-7389

CONCLUSION

The solid solution area in the phase diagram can be described by the combination of $Bi_3Zn_{2-x}Ta_3O_{14-x}$ and $Bi_{3+y}Zn_2Ta_{3-y}O_{14-y}$, to yield the formula $Bi_{3+y}Zn_{2-x}Ta_{3-y}O_{14-x-y}$, $-0.20 \leq y \leq 0.16$ and $0.00 \leq x \leq 0.40$. Solid solution series at $x = 0$ and $y = 0$ appeared to be dielectric and ε' range from 39 to 65.

ACKNOWLEDGEMENT

Special thanks are due to Ministry of Science, Technology, and Innovation Malaysia (MOSTI) for financial support via IRPA Grant and NSF scholarship.

REFERENCES

[1]. Boivin, J.C., and Mairesse, G. (1998); *Chem. Mater.* **10**, 2870.
[2]. Kayed, T.S., and Mergen, A. (2003); *Crystall. Res. Tech.* **38**, 1077.
[3]. Wang, H., Du, H., and Yao, X. (2003); *Materials Science and Engineering* **B99**, 20.
[4]. Mergen A., and Lee, W.H. (1997); *Mater. Res. Bull*. **32**, 175.
[5]. Matjaz, V., and Peter, K.D. (2000); *J. Am. Ceram. Soc*. **83**, 147.
[6]. Randall, C.A., Nino, J.C., Baker, A., Youn, H-J., Hitomi, A., Thayer, R., Edge, L.E., Sogabe, T., Anderson, D., Shrout, T.R., Trolier-Mckinstry, S., and Lanagan, M.T. (2003); *Am. Ceram. Soc. Bull.*,9101.
[7]. Youn, H.J., Sogabe, T., Randall, C.A., Shrout, T.R., and Lanagan, M.T. (2001); *J. Am. Ceram. Soc*. **84**, 2557.
[8]. Youn, H.J., Randall, C., Chen, A., Shrout, T., and Lanagan, M.T. (2002); *J. Mater. Res.* **17**, 1502.
[9]. Tan, K.B., Lee, C.K., Zainal, Z., Miles, G.C., and West, A.R. (2005); *J. Mater. Chem.* **15**, 3501.
[10]. Nobre, M.A.L., and Lanfredi, S. (2003); *J. Phys. Chem. Solids* **64**, 2457.
[11]. Nobre, M.A.L., and Lanfredi, S. (2001); *Mater. Lett*. **47**, 362.
[12]. Du, H.L., and Yao, X. (2003); *Materials Science and Engineering* **B00**, 1.

Corresponding Author: khaw.cc@gmail.com